CELL CYCLE
2018, VOL. 17, NO. 7, 844–857
https://doi.org/10.1080/15384101.2018.1456601

Taylor & Francis
Taylor & Francis Group

REPORT

Degraded melanocores are incompetent to protect epidermal keratinocytes against UV damage

Wen-Juan Yi, Meng-Yun Su, Ying Shi, Shan Jiang, Shi-Zheng Xu and Tie-Chi Lei

Department of Dermatology, Renmin Hospital of Wuhan University, Wuhan 430060, China

ABSTRACT

Melanosomes are membrane-bound intracellular organelles that are uniquely generated by melanocytes (MCs) in the basal layer of human epidermis. Highly pigmented mature melanosomes are transferred from MCs to keratinocytes (KCs), and then positioned in the supra-nuclear region to ensure protection against ultraviolet radiation (UVR). However, the molecular mechanism underlying melanosome (or melanin pigment) transfer remains enigmatic. Emerging evidence shows that exo-/endo-cytosis of the melanosome core (termed melanocore) has been considered as the main transfer manner between MCs and KCs. As KCs in the skin migrate up from the basal layer and undergo terminal differentiation, the melanocores they have taken up from MCs are subjected to degradation. In this study, we isolated individual melanocores from human MCs in culture and then induced their destruction/disruption using a physical approach. The results demonstrate that the ultrastructural integrity of melanocores is essential for their antioxidant and photoprotective properties. In addition, we also show that cathepsin V (CTSV), a lysosomal acid protease, is involved in melanocore degradation in calcium-induced differentiated KCs and is also suppressed in KCs following exposure to UVA or UVB radiation. Thus, our study demonstrates that change in the proportion of melanocores in the intact/undegraded state by CTSV-related degradation in KCs affects photoprotection of the skin.

Abbreviations: MCs: melanocytes; KCs: keratinocytes; HDFBs: human dermal fibroblasts; CTSV: cathepsin V; UVR: ultraviolet radiation; ROS: reactive oxygen species; ESR: electron spin resonance; DMPO: 5,5-dimethyl-1-pyrroline-N-oxide; TEM: transmission electron microscopy; CPDs: cyclobutane pyrimidine dimers; 8-oxo-dG: 8-oxo-2-deoxyguanosine; BCC: basal cell carcinoma; SCC: squamous cell carcinoma; FBS: fetal bovine serum; DMEM: Dulbecco's modified Eagle medium; LMA: low-melting-point agarose; NMA: normal-melting-point agarose; PBS: phosphate buffered saline; siRNA: small interfering RNA; SDS-PAGE: sodium dodecyl sulfate polyacrylamide gel electrophoresis.

ARTICLE HISTORY
Received 13 October 2017
Revised 20 February 2018
Accepted 19 March 2018

KEY WORDS
Melanocore; degradation; ultraviolet; cathepsin V; photoprotection; antioxidation

Introduction

Ultraviolet radiation (UVR) has been considered as the major environmental risk factor for skin photodamage (sunburn) and photoaging and even for photocarcinogenesis [1]. Solar UV rays that reach the earth's surface contain approximately 95% UVA (320-400 nm) and 5% UVB (280-320 nm). It is beyond dispute that most cases of skin cancer, such as basal cell carcinoma (BCC), squamous cell carcinoma (SCC) and malignant melanoma, are caused by excessive exposure to solar UVR, particularly its highly energetic UVB component [2,3]. However, human epidermis is fully equipped with a photoprotective defense mechanism to avoid/minimize the deleterious effects of UVR on the skin, to prevent cellular DNA damage and to scavenge harmful free radicals [4]. The following cellular events responsible for photoprotection have been studied extensively in skin exposed to UVR, including: 1) active melanin production in melanocytes (MCs) resulting from the up-regulation of tyrosinase activity; 2) the acceleration of melanosome transfer from MCs to neighboring keratinocytes (KCs), and 3) the subcellular localization of transferred melanosomes within KCs to form a supranuclear cap that serves as a shield to protect DNA against UVR [5,6]. Despite impressive advance in such fields of melanocyte research, the difficulty in monitoring the dynamic process of melanosome degradation both in undifferentiated and in differentiated KCs represents a major challenge to identify the photoprotective differences afforded by degraded or intact melanosomes [7–9].

Histological observations show that melanin granules are scarce in the Malpighian layer and the superficial cornified (horny) layer, whereas they are abundant in the basal layer. This suggests that melanin and melanosomes are degraded during their transit upward to the surface of the epidermis [10,11]. The prevalent mode of transfer between MCs and KCs through exo-/endo-cytosis of the melanosome core (termed melanocore) has been considered as the main manner in physiological context, melanocores in the recipient KCs actually reveal the absence of a melanosomal outer membrane [12]. It is not entirely clear what impact melanocore degradation has on protecting undifferentiated and/or differentiated KCs from UVR damage since studies to address this question have produced conflicting results. Jimbow and colleagues put forth the

CONTACT Tie-Chi Lei tchlei@whu.edu.cn 238#, Jiefang Road, Wuchang District, Wuhan 430060, China

interesting hypothesis that melanocore degradation appears to involve the reduction of melanocores into finer particles that may increase its effectiveness in shielding against UVR and in scavenging reactive oxygen species (ROS) [10]. However, recently published reports differ from that assumption in that the degradation and/or disintegration of melanocores causes them to lose their ROS scavenging activity [13] and their optical scattering properties [14]. To better understand whether the degradation of melanocores directly affects their photoprotective and anti-oxidant properties, in this study, we subjected human melanocores to physical destruction in an experimental model to simulate the degradation that may occur within KCs. We then analyzed their ability to photoprotect against UVR-induced DNA damage in treated (broken) or untreated (intact) melanocore-incorporated KCs following UVR. Using the electron spin resonance (ESR) spin-trapping technique, we also examined the ability of treated or untreated melanocores to inhibit the iron ion-catalyzed free radical decomposition of hydrogen peroxide using the Fenton reaction. In addition, we also showed that cathepsin V/L2 (CTSV), a lysosomal acid protease, is upregulated in calcium-induced differentiated KCs and suppressed in UVR-exposed KCs to increase the ratio of intact vs. broken melanocores, which potentially confers a stronger protection against UVR [15,16]. Our findings provide evidences for the first time that the photoprotective properties of melanocores are significantly improved in UVR-exposed KCs through the suppressed degradation of melanocores by the down-regulation of CTSV, which may be important for the design of new therapeutic approaches to protect against skin photoinjuries after exposure to sunlight.

Results

Loss of photoprotection against UVA and UVB in damaged melanocore-incorporated KCs

Equal amounts of melanocores isolated from human MCs and MNT1 cells were treated with multiple freeze-thaw cycles and manual grinding to physically damage them. Afterward, the treated (broken) or untreated (intact) melanocores were incubated with human KCs for 48 h to allow melanocores to be incorporated into KCs by phagocytosis. Upon examination using bright-field microscope, it was observed that melanocores predominantly aggregated in the perinuclear area, even forming a microparasol structure in keratinocytes exposed to 3 mJ/cm^2 UVB irradiation (Figure 1C). In comparison to the melanosomes in cultured melanocytes, melanocores purified from MCs revealed the absence of a melanosomal outer membrane (Figure 1A) [17]. Two specific antibodies against melanosome membrane marker (tyrosinase) and the amyloid fibril components within melanocores (Pmel 17/gp100) were used in western blotting to examine their corresponding protein levels in the melanocore-incorporated keratinocytes. As compared with the cultured melanocytes, the melanocore-incorporated keratinocytes exhibited significantly lower levels of tyrosinase, while Pmel 17/gp100 levels stayed relatively the same (Figure 1B). The melanocore-incorporated KCs were then irradiated with 3 J/cm^2 UVA or with 30 mJ/cm^2 UVB. DNA damage at the single cell level was detected using the comet assay (also called single-cell gel electrophoresis). The comet assay data showed that the percentage of DNA in the comet tail is higher in treated broken melanocore-incorporated KCs than in untreated intact melanocore-incorporated KCs following UV radiation (Figure 2), especially in UVB-exposed KCs ($P<0.05$). The two major DNA photoproducts, 8-oxo-dG (8-oxo-2-deoxyguanosine) and CPDs (cyclobutane pyrimidine dimers), induced by UVA and UVB radiation were also examined using immunofluorescence staining analysis (Figure 3). The immunofluorescent intensities of 8-oxo-dG and CPDs were significantly increased in damaged melanocore-incorporated KCs compared with intact melanocore-incorporated cells after UVA and UVB irradiation (Figure 3B). The results indicate that the ultrastructural integrity of melanocores taken up by KCs is of central importance to their photoprotective properties.

Loss of scavenging capacity for free hydroxyl radicals by damaged melanocores

To determine whether melanocore destruction affects their antioxidant properties, DMPO spin adducts were quantified in which hydroxyl radicals were generated by the Fenton reaction in the presence of untreated/intact or treated/broken melanocores obtained from primary MCs (Figures 4A, 4B). Compared to broken melanocores, untreated melanocores had markedly reduced amounts of DMPO-OH (Figure 4C, $P < 0.05$). These observations suggest that degraded melanocores become less effective in performing their antioxidant function.

Proteolytic effect of CTSV in KCs on melanocore degradation

To gain more insight about the role of CTSV in melanocore degradation in KCs, HaCaT cells were transfected with CTSV siRNA to silence CTSV mRNA expression and to suppress CTSV protein levels (Figure 5A). We purified melanocores from human MCs and then incubated melanocore specimens with CTSV-knockdown KC lysates in a slightly acidic (pH 5.5) environment. The ultrastructural changes of melanocores assessed by TEM are shown in Figure 5B. Most of the contour lines of melanocores remained visible in preparations treated with the CTSV-knockdown KC lysates. However, in sharp contrast, marked ruptures or disintegrations of the melanocores were found in the scrambled control. The percentage of damaged melanocores was significantly higher in the scrambled control (62%) than in the CTSV-knockdown KCs (31%) (Figure 5C, $P <0.05$). The CTSV-knockdown KCs also exhibited a much lower CTSV catalytic activity than that in the scrambled control (Figure 5E). Finally, we directly treated melanocore specimens with commercially available recombinant human CTSV (rhCTSV). The ultrastructural changes in rhCTSV-treated melanocores were very similar to those treated by KC lysates obtained from the scrambled control siRNA. However, heat-inactivated CTSV had no discernible activity on melanocores (Figures 5B and 5D). These findings collectively suggest that the expression of CTSV in KCs contributes to the breakdown of the protein components in the melanocores.

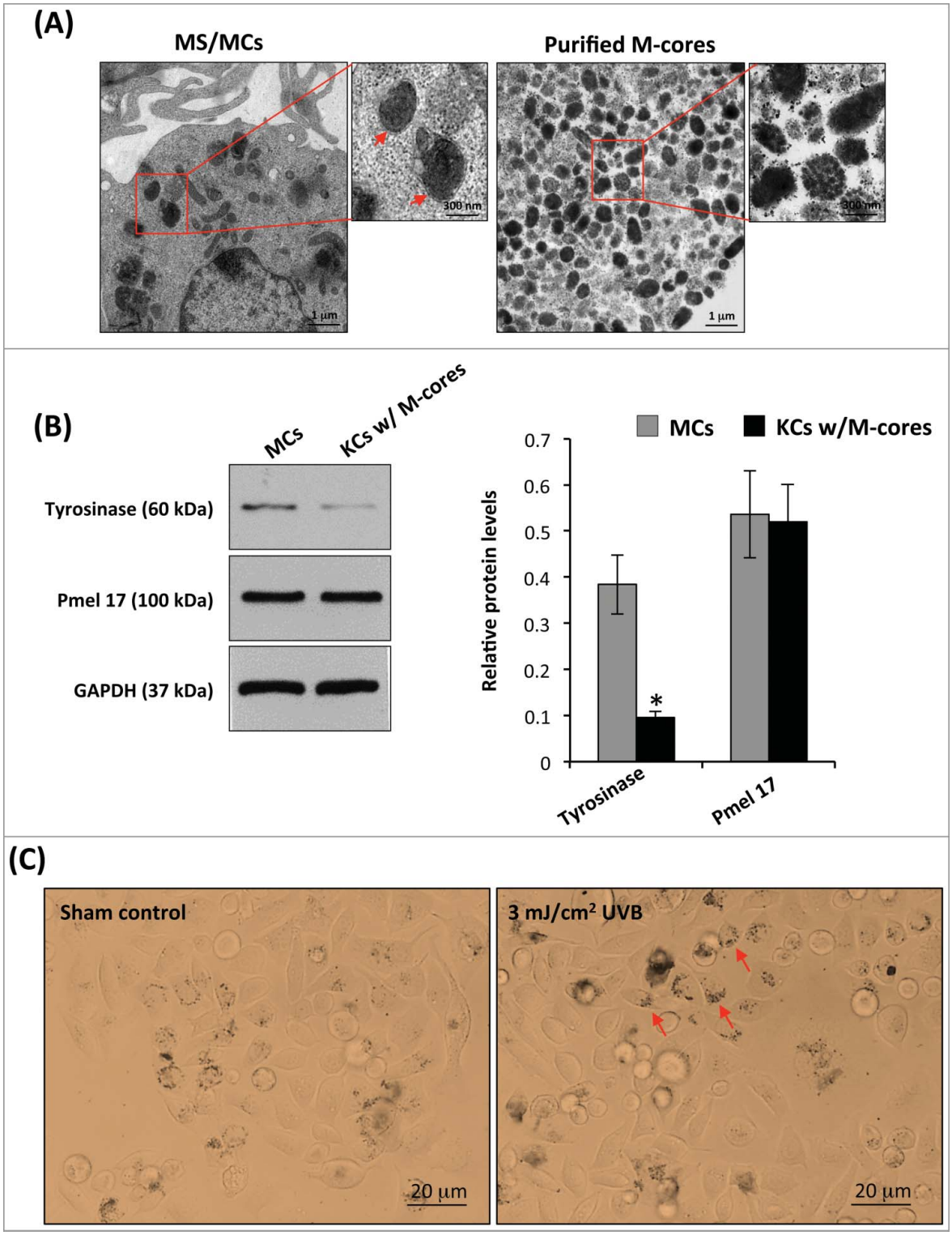

Figure 1. Isolation and characterization of melanocores. (A) Melanocores (M-cores) were isolated from normal human MCs and MNT1 melanoma cells as described in the *Materials and Methods*. The melanocore pellets were examined by TEM. The representative TEM micrograph on the right panel shows the melanocores characteristic absence of the outer envelope membrane. Melanosomes in a normal MC are shown on the left panel, the red arrows indicate the visible outer membrane. Higher magnifications of the boxed areas in each low-power image are shown on the right. (B) Purified melanoscores were incubated with human KCs for 48 h to allow for a more efficient uptake of melanocores by KC. The cells were washed with warm PBS to remove the unincorporated melanocores and lysed in extraction buffer. Two antibodies against tyrosinase (a melanosomal membrane marker) and Pmel 17/gp100 (the intraluminal amyloid fibrils) were used in western blotting to examine their corresponding protein levels. The histogram (on the right) shows the densitometric quantification of data with means ± SD of 3 independent experiments. (C) Purified melanocores were incubated with human KCs for 48h. The distribution of melanocores, in unexposed or 3 mJ/cm^2 UVB-exposed KCs, was examined using the bright-field microscopy, arrows indicate the microparosol formation.

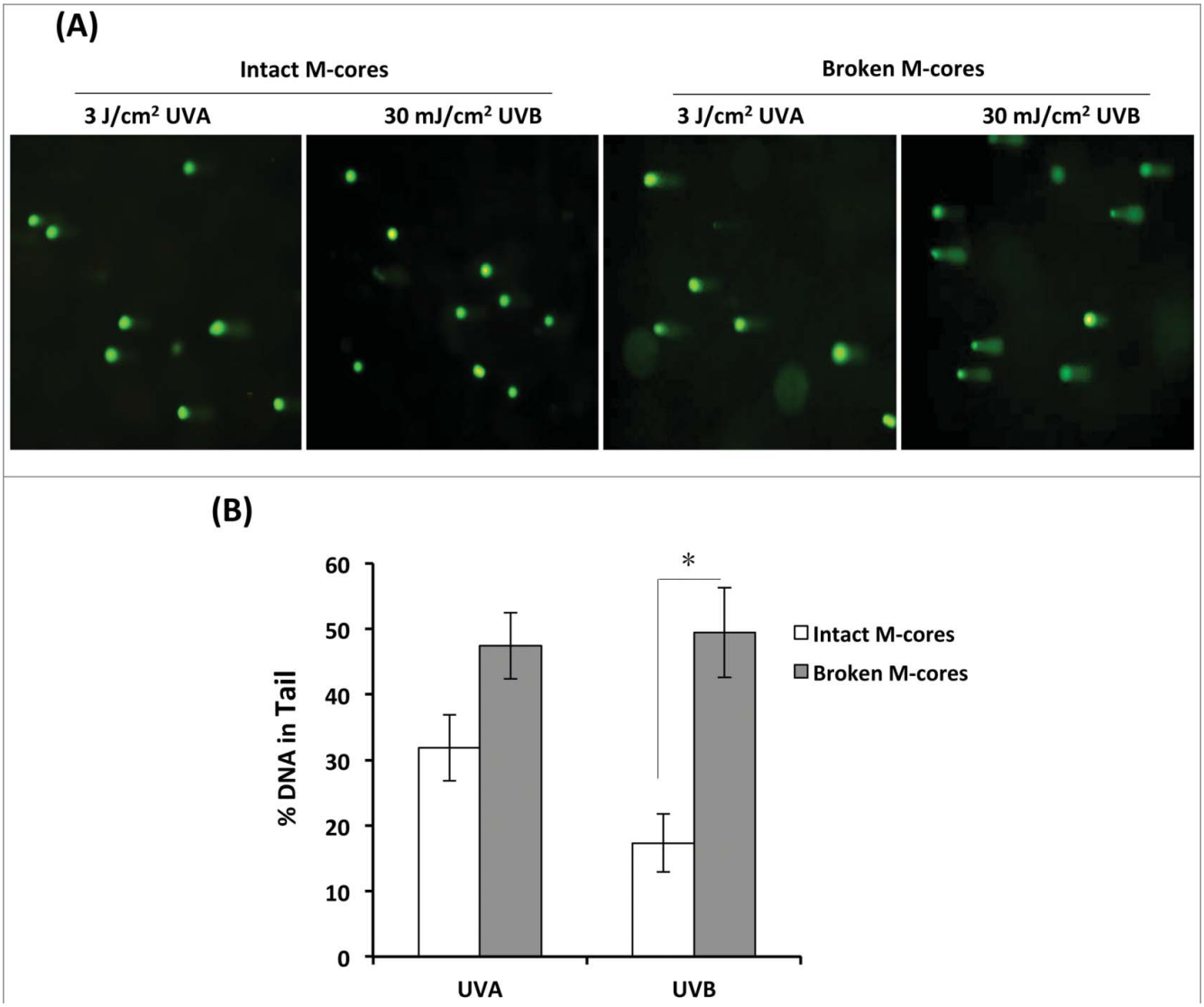

Figure 2. Damaged melanocores are incompetent to protect keratinocytes against UVA or UVB photodamage. (A) KCs were seeded into 6-well culture plates at 2×10^4 cells per well and were cultured overnight to attach to the cell plates. Purified melanocores were subjected to destruction by a physical procedure. Equal amounts (ranging from 1,000 to 2,000 melanocores per well) of treated (broken) or untreated (intact) melanocores were then dropped on each cell culture. Following an incubation time of 48 h, the cultures were washed using warm PBS and then directly irradiated with 3 J/cm^2 UVA or 30 mJ/cm^2 UVB, and comet assays were performed to measure DNA damage in individual cells. Images of comet tail DNA in representative cells exposed to UVA or UVB are shown. (B) The bar graphs show the mean comet percentage of tail DNA (%Tail DNA) from 3 independent experiments with at least five fields of 100 cells counted per experiment. $^*P < 0.05$.

Up-regulation of CTSV in calcium-induced KCs differentiation increases melanocore degradation

The most recent articles reported by *Correia* and *Hurbain* show that transferred melanocores are kept in a non-acidic or/ non-degradative compartment of the keratinocytes [12,18]. To explain this discrepancy between our observation and these published results, we increased calcium concentration in the cultured medium in order to induce keratinocyte differentiation. The results indicated that there were significant upregulations of CTSV protein and mRNA in 1.3 mM calcium-treated keratinocytes as compared with those in 0.06 mM calcium-treated cells (Figure 6A). The western blotting analyses with Pmel 17/gp100 antibody revealed that there was a significant decrease in Pmel 17 protein level in the keratinocytes treated with 1.3mM calcium for 72 h, and no change in the melanocores-incorporated fibroblasts (Figure 6C). In addition, we also used the siRNA technique to knock down the CTSV expression in KCs, which were then treated with 0.06 mM or 1.3 mM calcium and incubated with an equal amount of purified melanocores. The decreased Pmel 17/gp100 protein level was only detected in 1.3 mM calcium treated keratinocytes, while no change was found in 0.06 mM calcium treated cells (Figure 6B). Similar results were obtained from the chase assays (Figure 6C). These results showed that undifferentiated keratinocytes did not influence the degradation of incorporated melanocores. Calcium-induced differentiated keratinocytes particularly degrade incorporated extrinsic melanocores.

Down-regulation of CTSV in UVA or UVB-exposed KCs suppresses melanocore degradation

CTSV mRNA and protein levels in HaCaT cells exposed to UVA (3-30 J/cm^2) or to UVB (10-100 mJ/cm^2) were

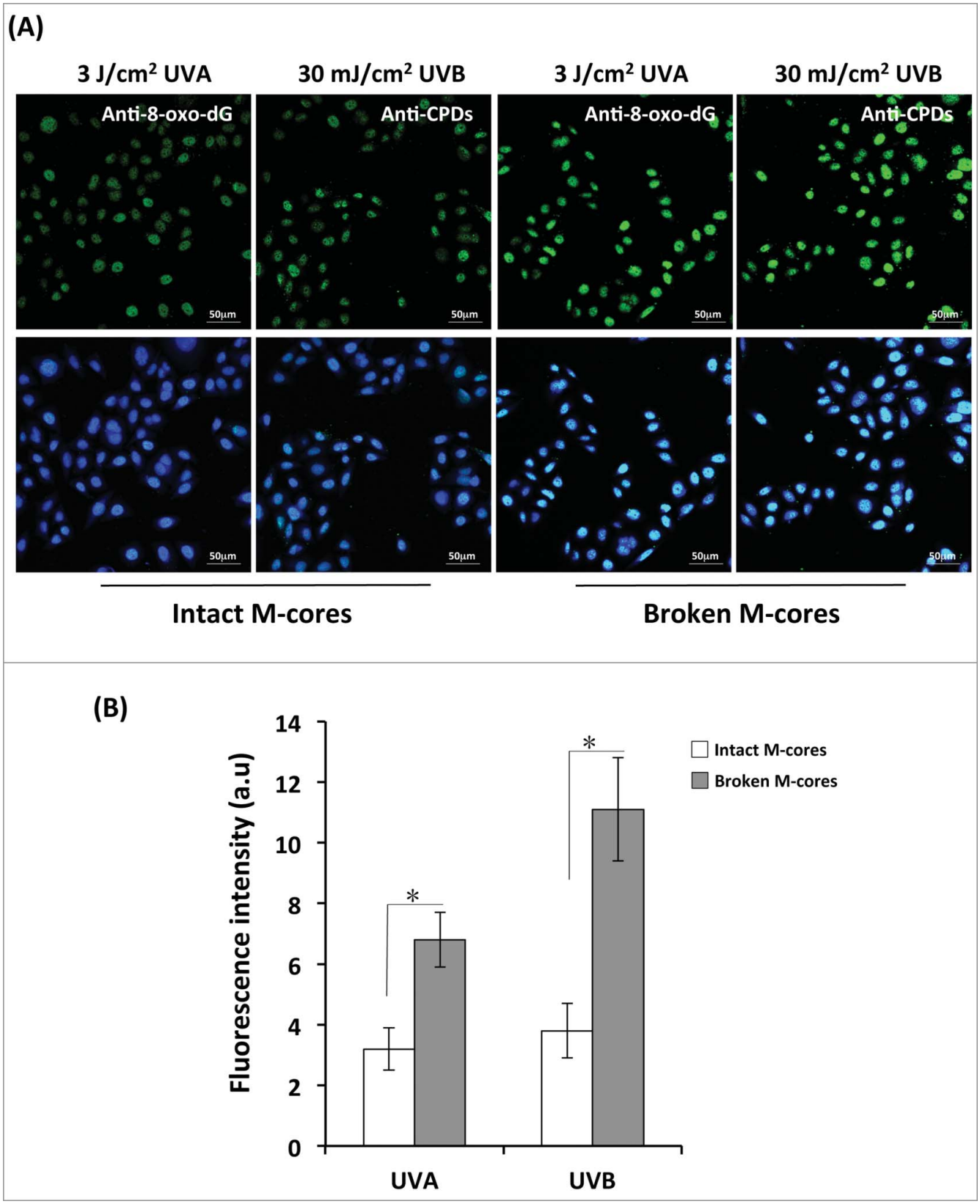

Figure 3. Determination of 8-oxo-dG and CPDs formation by immunofluorescence staining. (A) KCs were loaded with treated (broken) or untreated (intact) melanocores as described for Figure 2 and were grown on coverslips and irradiated with 3 J/cm^2 UVA or 30 mJ/cm^2 UVB. The cells were immediately fixed in 4% paraformaldehyde in PBS, and were then immunostained with antibodies to CPD and to 8-oxo-dG. The slides were counter-stained with DAPI to identify nuclei (blue). Staining was observed using an Olympus FV1200 confocal fluorescence microscope. Representative fluorescence images of 8-oxo-dG and CPDs are shown in the upper row. Merged images including DAPI-staining of nuclei (blue) are shown in the bottom row. Scale bar: 50 μm. (B) Mean intensities of 8-oxo-dG and of CPDs quantified using Image J software; bars show means $\pm$ SD of intensities from 3 independent experiments. $^{*}P < 0.05$.

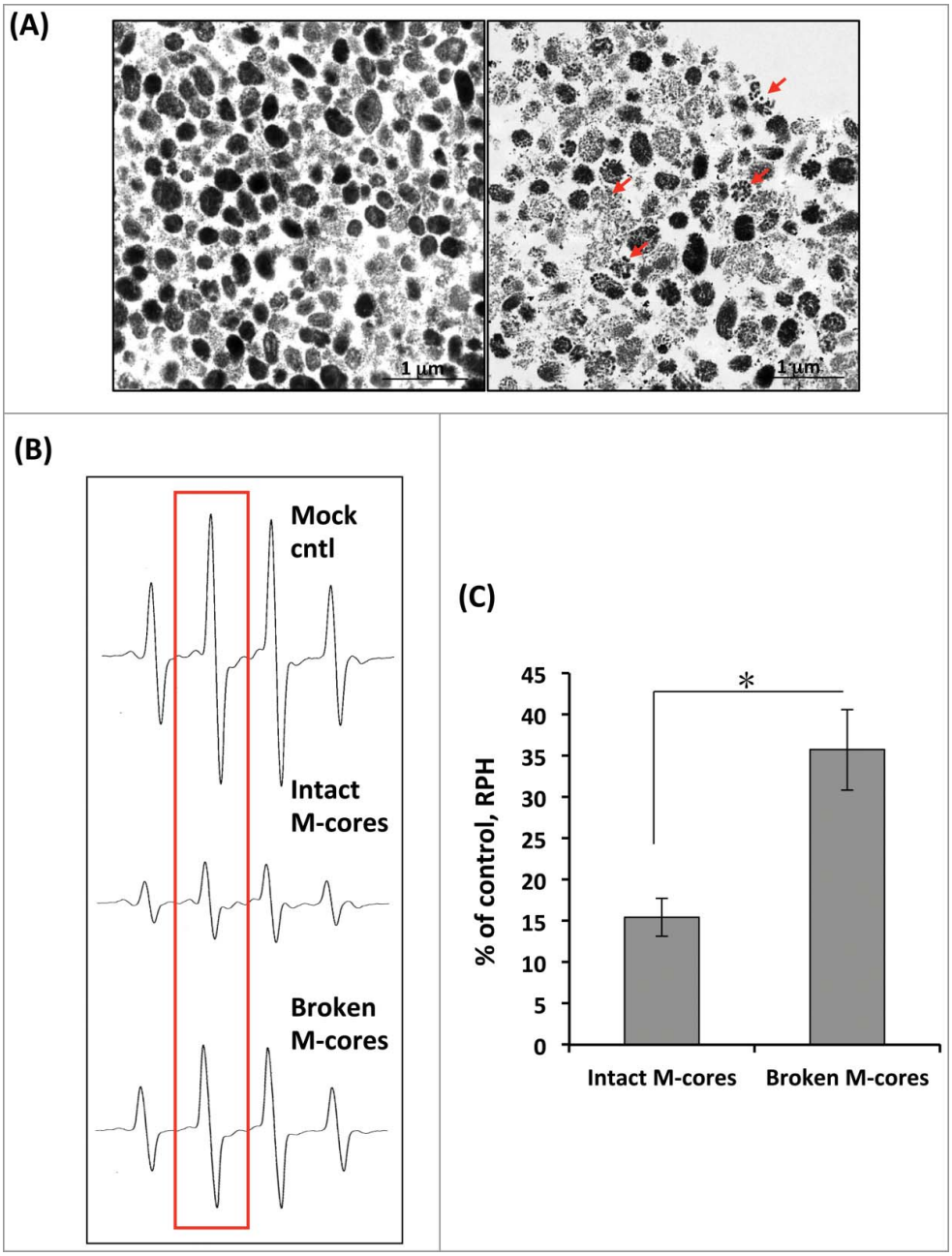

Figure 4. Effects of treated (broken) and untreated (intact) melanocores on hydroxyl radical generation in the Fenton reaction. (A) Individual melanocores were isolated from primary MCs and were then subjected to destruction by a physical procedure as described in the *Materials and Methods*. The ultrastructural integrity of melanocores was examined by TEM. Representative TEM images show that untreated melanocores (left panel) are oval-shaped or round with an apparent contour line, while treated melanocores (right panel) seem to be disintegrated or fragmented, as indicated by the arrows. (B) Representative ESR spectra of DMPO–OH with treated or untreated melanocores. Hydroxyl radicals are generated by the Fenton reaction (DMPO: 400 mM). (C) Comparison of hydroxyl radical-scavenging activity for treated or untreated melanocore specimens. Student's unpaired t-test was used to determine the statistical difference between treated melanocores and the untreated control. $^{*}P < 0.05$.

dramatically decreased in a UV dose-dependent manner (Figures 7A and 7B). The changes in CTSV enzyme activity were very similar to its transcript levels (Figure 7E). Additionally, we examined the ultrastructural changes of melanocores treated with cell lysates derived from UVB-exposed and from unexposed KCs. The percentage of damaged melanocores was significantly higher in the unexposed controls (45%) than in the UVB-treated group (29%) (Figures 7C and 7D, $P < 0.05$). These results demonstrate that the suppression of CTSV activity in KCs by UV radiation could repress melanocore degradation.

Discussion

Here, we report that the ultrastructural integrity of melanocores in recipient KCs is necessary for their crucial photoprotective role due to their optical properties (absorption, reflection and scattering) [19] and to their anti-oxidative properties [20]. The data obtained from the comet assay and immunofluorescent staining of UV-specific photoproducts (8-oxo-dG for UVA and CPDs for UVB) indicated that DNA damage and UV-signature mutations are more severe in broken-melanocore incorporated KCs than in intact-melanocore incorporated KCs following

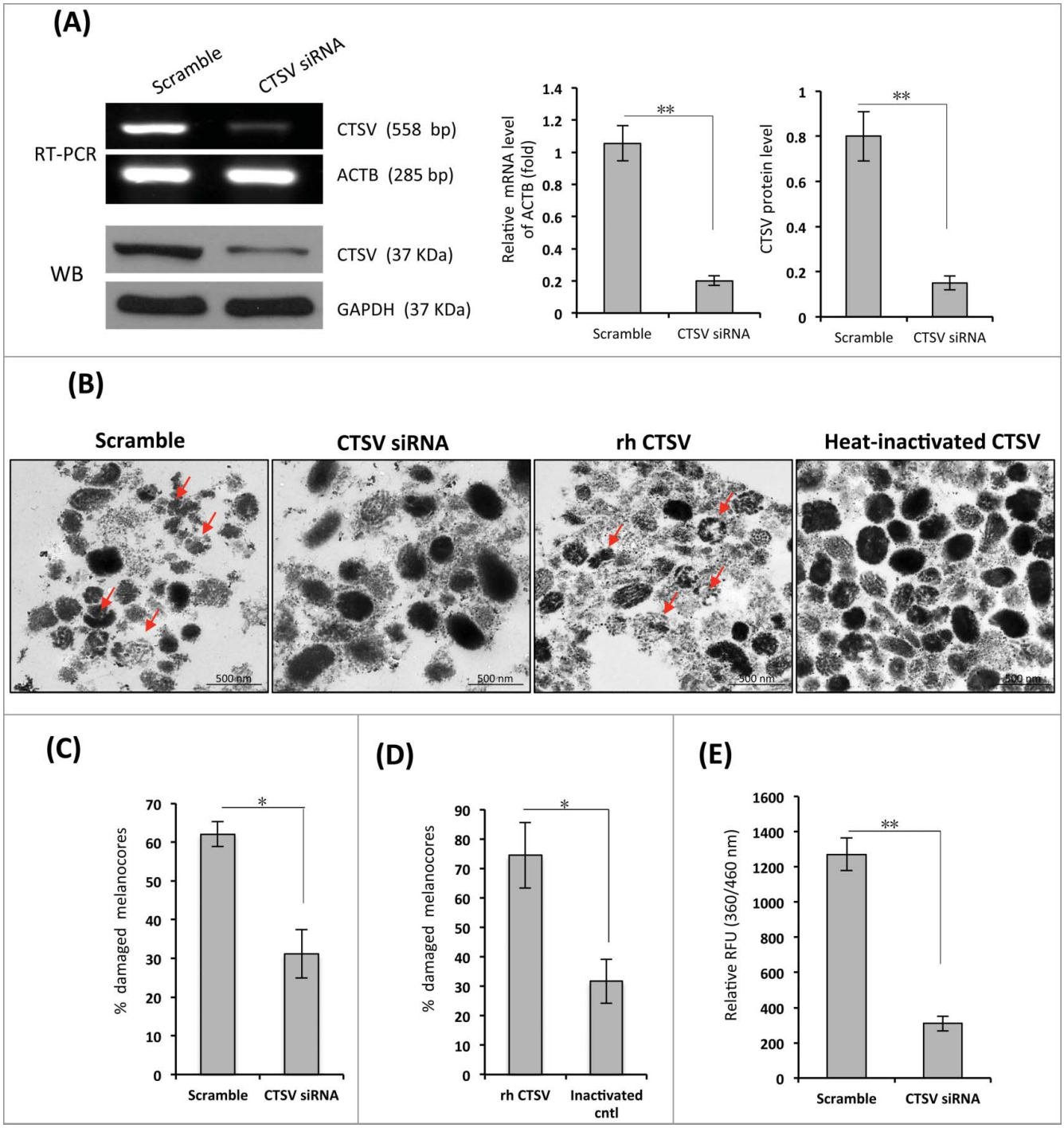

Figure 5. Effects of siRNA-mediated knockdown of CTSV in KCs on melanocore degradation. (A) HaCaT cells were transfected with CTSV siRNA or the scrambled control for 72 h. The efficiency of CTSV knockdown by these siRNAs was tested using western blotting and RT-PCR. The histogram (on the right) shows the densitometric quantification of data with means ± SD of 3 independent experiments. (B) Cell lysates were prepared from siRNA-transfected HaCaT as noted, and individual melanocores were isolated from human MCs in culture, as described in the *Materials and Methods*. The melanocore specimens were incubated with the cell lysates at 37°C for 8 h. Representative TEM images show that lysates of CTSV-transfected HaCaT cells have less of a destructive effect on melanocores than lysates of the scrambled control, as indicated by the arrows (shown on the left). The melanocore specimens were also incubated with 1 μg/mL rhCTSV or a heat-inactivated control; TEM images are shown on the right. (C and D) Comparison of percentages of damaged melanocores from 3 independent experiments. $^{*}P < 0.05$. (E) CTSV enzyme activity of cell lysates was estimated using the fluorogenic dipeptide substrate Z-Leu-Arg-AMC. The histogram shows the means ± SD of fluorescence intensities from 3 independent experiments. $^{*}P < 0.05$, $^{**}P < 0.01$.

UVR (Figures 2 and 3). ESR spin-trapping analysis provided direct evidence that broken-melanocores exhibited a decreased scavenging effect on free hydroxyl radicals compared to intact untreated melanocores (Figure 4). Our findings suggest that melanocore degradation is a previously unappreciated process responsible for the regulation of cutaneous photoprotective capacity.

Emerging evidences show that melanin granules reside in a poor hydrolytic/non-acidic compartment in keratinocytes to prevent rapid degradation [12,18]. Another recent study

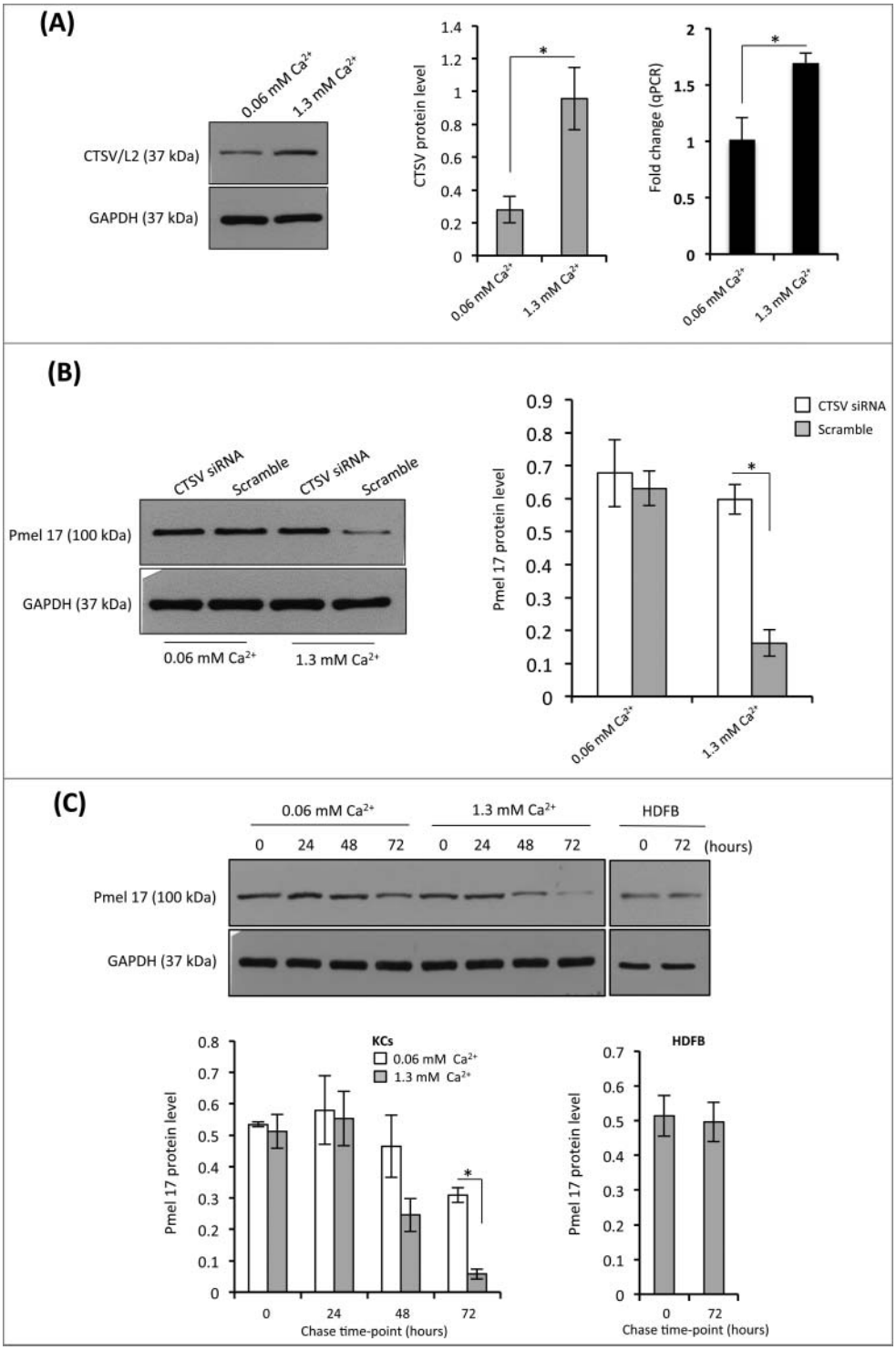

Figure 6. Melanocore degradation is sensitive to CTSV up-expression in Ca^{2+}-induced differentiated KCs. (A) Human KCs were cultured with EpiLife medium supplemented with 0.06 mM or 1.3 mM calcium for 48 h. The total RNA or protein was extracted from cultured cells, the mRNA and protein level were detected using qPCR and western blotting, respectively. Representative blot is shown on the left, the densitometric quantification of the intensity of the bands is shown on the middle. The levels of CTSV mRNA are shown on the right. $^{*}P < 0.05$. (B) KCs were transfected with CTSV siRNA or the scrambled control for 72 h in the medium containing 0.06 mM or 1.3 mM calcium, as described for Figure 5. The cells were incubated with equal amount of melanocores for 72 h. The melanocore-incorporated KCs were harvested for the determination of Pmel 17/gp100 protein. Representative blot is shown on the left, the histogram (on the right) shows the densitometric quantification of data with means ± SD of 3 independent experiments. $^{*}P < 0.05$. (C) The melanocore-incorporated KCs were cultured in the medium containing 0.06 mM or 1.3 mM calcium for varying time points (0, 24, 48, and 72h). The cells were harvested for chase analysis of Pmel 17/gp100 protein. The histogram (on the left) shows the densitometric quantification of data with means ± SD of 3 independent experiments. Human dermal fibroblasts (HDFBs) as a control are shown on the right. $^{*}P < 0.05$.

showed that lysosome inhibitors (E-64-D and pepstatin A) significantly increased the accumulation of melanosomal protein Pmel 17 in the melanocore-incorporated keratinocytes. They also found that this lysosomal degradation of melanosomes did not influence the early phase of incorporation, i.e., the phagocytic or endocytic processes [21]. CTSV (EC: 3.4.22.43) is a lysosomal acid protease. We observed an upregulation of CTSV protein and mRNA in 1.3 mM calcium-treated keratinocytes as

compared with those in 0.06 mM calcium-treated cells (Figure 6A). Other investigators have already characterized the detailed tissue distribution of CTSV using an ultrathin cryosection combined with immunogold labeling. Their results revealed that CTSV was expressed predominantly within the stratum spinosum and stratum corneum of the epidermis, and to a lesser degree in the basal layer [15,18]. Based on these findings, we hypothesized that melanocores are initially endocytosed and reside in the non-degradative compartments of undifferentiated basal keratinocytes in order to avoid premature degradation. However, these melanin-loaded compartments within differentiated keratinocytes likely fuse with CTSV-enriched lysosomes through the autophagic/lysosomal pathway [21], and as a result are subjected to the breakdown of the protein components within the melanocores.

To gain more insight about the role of CTSV in melanocore degradation, we examined the effects of CTSV-siRNA knockdown KC lysates on melanocore ultrastructure compared with the scrambled control siRNA group. The results (Figure 6) show that gene silencing of CTSV by siRNA in KCs results in the reduction of melanocore degradation. Similar ultrastructural changes were also observed in melanocore specimens treated directly with commercially available recombinant human CTSV enzyme. These data suggest that the enzyme activity of CTSV in KCs contributes to melanocore degradation. Furthermore, we examined the levels of CTSV mRNA and protein in UVA-/UVB-induced HaCaT cells using Western blotting and qPCR assays. The results show that CTSV protein and mRNA transcript levels in cells exposed to UVR decreased in a UVR dose-dependent manner (Figure 7). The cell lysates derived from UVB-exposed KCs revealed a reduced melanocore degradation capacity compared to the unexposed controls. These findings suggest that the increased proportion of melanocores in the intact and undegraded state enhances the skin photoprotective function.

Taken together, our results provide new insight into the fate and functions of transferred melanosomes in KCs and answer the long-standing question of whether the ultrastructural integrity of melanosomes is required to perform their photoprotective function. The proteolytic degradation of melanosomes by CTSV occurs preferentially in the differentiated compartment of the skin, serving as a potential mechanism against the premature degradation of newly transferred melanosomes in the proliferating basal cell compartment since these intact melanosomes are more effective in preventing photodamage. Hence, the modulation of melanosome degradation represents an attractive therapeutic target for controlling skin cancer, especially under intensive sunlight exposure.

Materials and methods

Cell cultures, calcium-induced KC differentiation and UVA/UVB radiation

Primary human epidermal MCs, human epidermal KCs, and human dermal fibroblasts (HDFBs) were isolated from juvenile foreskin tissues (skin phototype III/IV) as previously described [22,23] with a minor modification. MCs and KCs were cultured with complete Medium 254 and EpiLife medium, respectively, (all from Cascade Biologics, Portland, OR, USA). All cells used in our experiments were from passages 2 to 4. To induce KC differentiation, KCs were cultured in the Epilife medium supplemented with 0.06 mM calcium or 1.3 mM calcium, as described previously [24]. HaCaT cells (human immortalized KCs), HeLa cells (human cervical carcinoma cell) were purchased from the China Center for Type Culture Collection (Wuhan, China) and were routinely cultured in DMEM (Gibco, Invitrogen, Carlsbad, CA, USA) with 10% fetal bovine serum (FBS, HyClone, Logan, UT, USA). In some experiments, HaCaT were also grown in complete EpiLife medium. MNT1 human melanoma cells were generously provided by Dr. Vince Hearing (Pigment Cell Biology Section, NCI, NIH, USA), and were grown in DMEM supplemented with 20% FBS. All cells were maintained at 37°C, 95% humidity and 5% CO_2. For UVA or UVB radiation, the cells were treated using a high dose targeted phototherapy system (Daavlin, Bryan, OH, USA) with a maximum wavelength at 350 or 311 nm, respectively. The dosage of UVR used is indicated in the Figure Legends.

Preparation and treatment of melanocore-enriched subcellular fractions

We used a previously described protocol to isolate the melanocore-rich fraction [25–27]. Briefly, confluent monolayers of human MCs or MNT1 were harvested and kept frozen at 2×10^6 cells per Eppendorf tube (1.5 mL). After thawing the frozen cells, 1 mL cold lysis buffer, consisting of 0.1 M Tris-HCl, pH 7.5, 1% Igepal CA-630 (Sigma-Aldrich, I3021) and 0.01% SDS, was added to the cells and was kept at 4°C for 20 min with mixing every 10 min. After centrifugation (1×10^3g for 5 min at 4°C), the supernatants were transferred to new Eppendorf tubes (1.5 mL) and were centrifuged again in the same manner. The supernatants were then further centrifuged (2×10^4g for 5 min at 4°C) and the precipitates were washed twice with D-PBS with brief and gentle mixing in order to avoid dispersion and were then centrifuged again (2×10^4 g for 5 min at 4°C). The ultrastructures of melanocore pellets were then examined using transmission electron microscope (TEM). To induce the melanocore degradation, the melanocore specimens were treated using the physical approach of multiple freeze-thaw cycles and manual grinding using a glass Dounce homogenizer (Wheaton, Millville, NJ, USA). The destruction/disruption of the treated melanocores was confirmed and imaged at the ultrastructural level using TEM.

Uptake and distribution of melanocores in KCs

Keratinocytes were incubated with melanocores isolated from human MCs or MNT1 as described previously [28,29]. KCs were plated at 2×10^4 cells per well in 6-well cell culture plates. Isolated melanocores were added at the same concentration per well. The treated (broken) or untreated (intact) melanocores were dropped on the cell cultures in excess, ranging from 1,000 to 2,000 melanocores per well. Following an incubation time of 48 h to allow melanocore uptake by KCs via phagocytosis, KCs were rigorously washed 3 times with 1 × PBS to remove the non-incorporated melanocores. The melanocore-incorporated KCs were further examined ultrastructurally as detailed below.

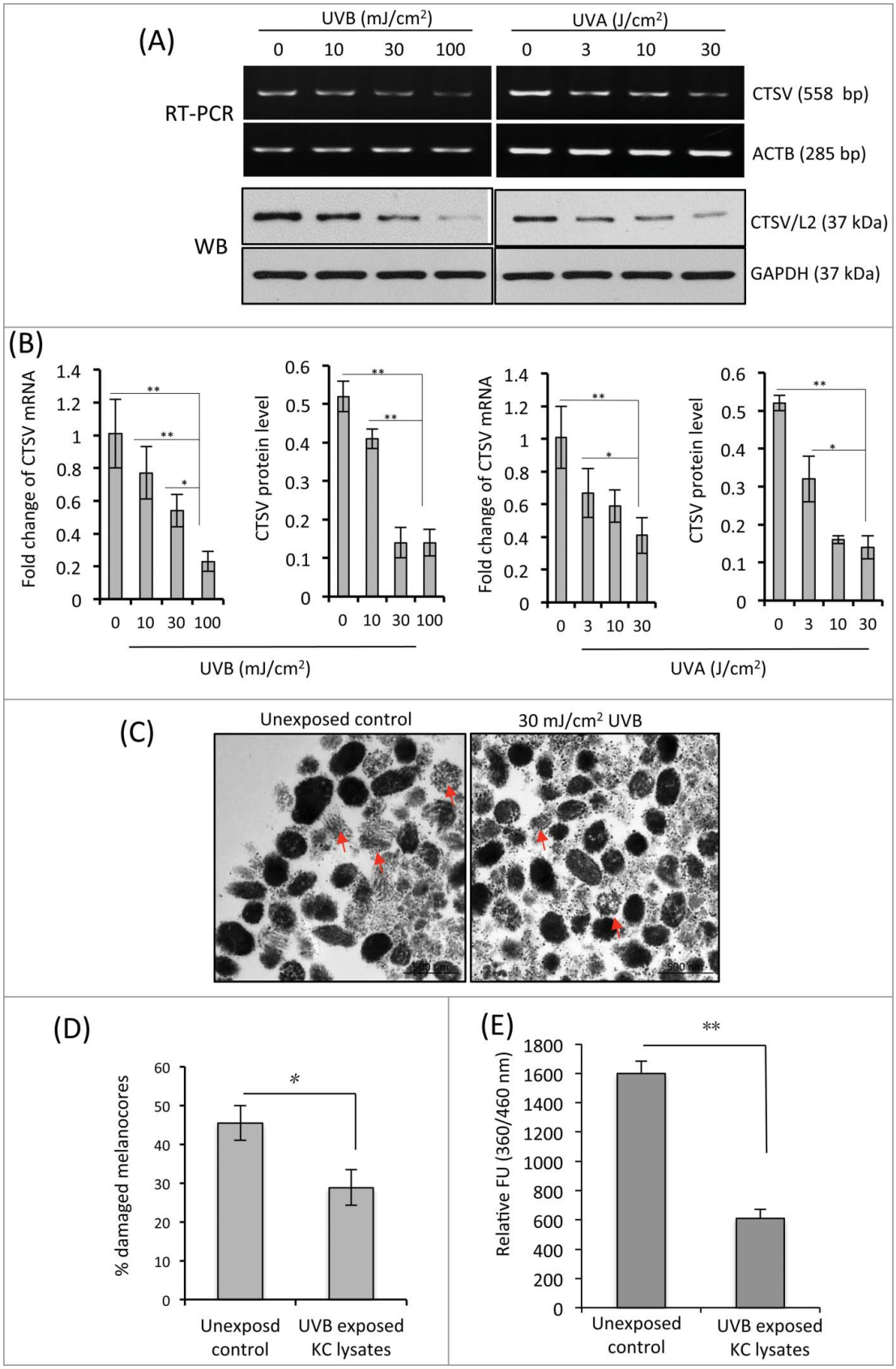

Figure 7. Suppression of CTSV mRNA and enzyme activity in KCs exposed to UVA or UVB. (A) HaCaT cells were seeded into 6-well cell culture plates and were irradiated with UVA (0, 3, 10 and 30 J/cm^2) or UVB (0, 10, 30 and 100 mJ/cm^2). The cells were harvested at 24 h post-irradiation. Protein and mRNA transcript levels of CTSV were determined by western-blotting and semi-quantitative RT-PCR, respectively. Representative images of 3 experiments are shown. (B) qPCR was performed to measure CTSV mRNA levels. The intensities of western-blot bands were quantified using Image J densitometry software. The levels of CTSV mRNA and protein are reported from 3 independent experiments. $^{*}P < 0.05$, $^{**}P < 0.01$. (C) Cell lysates were prepared from KCs exposed to 30 mJ/cm^2 UVB and then incubated with isolated melanocore specimens at 37°C for 8 h. Representative TEM images show that UVB-exposed KCs have less of a destructive effect on melanocores than the unexposed control, as indicated by the arrows. (D) Comparison of percentages of damaged melanocores from 3 independent experiments. $^{*}P < 0.05$. (E) Enzyme activity of CTSV in UVB-exposed keratinocyte lysates was estimated using the fluorogenic dipeptide substrate Z-Leu-Arg-AMC. Results are averages of 3 independent experiments. $^{**}P < 0.01$.

The melanocore distribution in KCs was examined using bright-field microscope.

Ultrastructural observations of melanocores by TEM

Cell samples and melanocore pellets were harvested and fixed with 2% glutaraldehyde in D-PBS at 4°C for at least 2 h. After washing twice with D-PBS for 15 min each, the cells were post-fixed with 2% osmium tetroxide for 1.5 h. After fixation, they were dehydrated in a graded series of ethanol and propylene oxide, and embedded in epoxy resin (EPON) for 48 h at 60°C. Ultrathin sections were cut and then stained with uranyl acetate and lead citrate and were examined using TEM (Tecnai G^2 20 TWIN, FEI, USA) at 200 kV. At least five TEM images were randomly taken of each melanocore specimen. The Image J software was used to quantify the grayscale values of the area bounded by contour lines of the melanocores or spreading area of the melanin pigment. The percentage of damaged melanocores was calculated to represent the efficacy of melanocore degradation [30].

Comet assay

The modified comet assay for KCs was carried out according to a previously described method [31]. KCs were co-cultured with intact or damaged melanocores for 48 h and then were exposed to UVA (3 J/cm^2) or UVB (30 mJ/cm^2). Immediately after UVA irradiation or 2 h after UVB irradiation, treated KCs were collected and suspended in PBS, 25 μl KCs (2×10^6 cells/mL, counted by the trypan blue method) were resuspended in 75 μl 0.75% low-melting-point agarose (LMA) in PBS then transferred onto frosted glass microscope slides precoated with 0.75% normal-melting-point agarose (NMA) (warmed at 37 °C prior to use), and then carefully covered with a coverglass at 4°C for 10 min. In other words, slides were precoated with the first layer of 0.75% NMA, then with a second layer of the cell suspension in 0.75% LMA, and then were coated with the third layer of 0.75% LMA, and stored at 4°C for 10 min to allow solidification. Finally, the coverglasses were removed, and the slides were immersed in lysis solution (2.5 mM NaCl, 100 mM Na_2EDTA, 10 mM Tris base (pH 10.0) and 1% Triton X-100) at 4°C for 1.5 h. After lysis, each slide was immersed in fresh electrophoresis solution (300 mM NaOH, 1 mM Na_2EDTA, pH 13.0) for 20 min to allow DNA unwinding and the expression of single-strand breaks and alkali-labile sites. Electrophoresis was conducted at 4°C for 20 min (25 V/300 mA). After electrophoresis, slides were neutralized (400 mM Tris, pH 7.5) and stained with Goldview (SBS Genetech Co., Ltd., Shanghai, China). The comet images were observed and photographed at 400 × magnifications using a fluorescence microscope (Olympus BX51, Japan). DNA damage was analyzed by CASP software (available at http://www.casp.of.pl). At least five fields of 100 cells were randomly selected of each sample. The percentage of DNA in the comet tails (%Tail DNA) was measured. To prevent additional DNA damage, all steps described above were performed under dimmed light.

Detection of DNA damage by immunofluorescent staining

Immunofluorescent staining of 8-oxo-dG and CPDs was performed as described previously [32]. Five × 10^4 KCs per ml were seeded into 6-well culture plates containing sterile coverslips. After overnight culture, the medium was replaced with fresh medium containing isolated melanocores. After an additional 48 h incubation, the cells were washed with warm PBS 3 times to remove non-incorporated melanocores, and the cells were then irradiated with 3 J/cm^2 UVA or 30 mJ/cm^2 UVB. The cells were immediately fixed in 4% paraformaldehyde in PBS for 15 min at room temperature, permeabilized with 0.5% Triton X-100/PBS for 15 min, followed by 3 washes with PBS. Two N HCl was added to each well for 30 min at 37°C and neutralized with 50 mM Tris base. The coverslips were rinsed 3 times with PBS and blocked with 10% normal goat serum for 1 h at 37°C. The primary antibodies, anti-CPD (Cat#: NMDND001, Cosmo Bio, Tokyo, Japan) or anti-8-oxo-dG (Cat#: 4354-MC-050, Trevigen, MD, USA), were diluted in antibody diluent buffer and were layered on the coverslips at 4°C for 16–18 h. The secondary antibody, goat anti-mouse IgG (H+L) conjugated with Alexa-488 (Invitrogen, Carlsbad, CA, USA), was diluted to 1:200 with antibody diluent buffer and was incubated with the cells on coverslips for 1 h at 37°C. The secondary antibody solution was then decanted and slides were washed 3 times with PBS for 5 min each in the dark. Mounting medium containing 4', 6-diamidino-2-phenylindole (DAPI) (1.5 μg/ml) (Vector Laboratories, Burlingame, CA, USA) was used for counterstaining. Images were obtained using a laser scanning confocal microscope (FV1200; Olympus Corporation, Tokyo, Japan). At least ten images were taken of each coverslip, and the mean intensity was measured in triplicate experiments. The mean intensities of 8-oxo-dG and CPDs were quantified using Image J software (NIH, Bethesda, MD, USA).

Fenton reaction and hydroxyl radical measurement using a spin trapping assay

The effects of melanocore specimens on hydroxyl radical (•OH) generation in the Fenton reaction were studied using a spin trapping method, according to our previous report [33]. $FeSO_4$ was dissolved in distilled water, while all other solutions were dissolved in 0.1 M phosphate buffer (pH 7.4). The spin trap compound 5,5-dimethyl-1-pyrroline-N-oxide (DMPO) was purchased from Sigma Chemical Co. (St. Louis, MO. Catalog# D5766). Each reaction was carried out in a total of 50 μl in an Eppendorf tube containing 260 mM H_2O_2, 0.4 mM $FeSO_4$, 400 mM DMPO and identical amounts of treated or untreated melanocores as noted. In the control, metal-free water was substituted for the sample. The Fenton reaction was initiated by the addition of H_2O_2, and then 50 μl of each reaction mixture was placed in an ESR quartz flat cell. Exactly 20 s after the addition of H_2O_2, the ESR spectra of the DMPO-•OH spin adducts were recorded at room temperature using a Bruker ER 200D-SRC ESR spectrometer (Bruker Analytische Messtechnik GmbH, Rheinstetten, Germany) operating at 9.53 GHz microwave frequency, 20 mW microwave power, 100 kHz modulation frequency and 0.05 mT modulation amplitude. •OH scavenging activity was calculated using the

equation: •OH scavenging activity = [1-(H/H_0)] × 100%, in which H and H_0 represent relative peak heights (amplitude) of the second peak of the DMPO-•OH spin adduct with or without sample, respectively.

Semi-quantitative RT-PCR and quantitative real-time PCR (qPCR)

Total RNAs were isolated from HaCaT or KCs using Trizol reagent (Invitrogen, Eugene, OR, USA) according to the instructions of the manufacturer. cDNAs were synthesized from total RNAs using a Moloney murine leukemia virus reverse transcriptase (M-MLV) first strand kit (Invitrogen, Shanghai, China). PCR was performed in triplicate with SYBR Green PCR core reagents (Applied Biosystems, Foster City, CA, USA), 50 ng cDNA, 1 μM forward and reverse primers for the CTSV gene (forward: 5'-TTCCGTGAGCCTCTGTTTCT-3'; reverse: 5'-CGAATTTGCTCCTTCAAAGC-3') or (forward: 5'-GGAAGG-CAACACACAGAAGA-3'; reverse: 5'-TGTTTCCCTTGGCTG-TATTC-3') were used to produce amplicons of 558 bp and 118 bp, respectively, for RT-PCR and qPCR. The housekeeping gene β-actin (ACTB) was used as an endogenous internal control (forward primer 5'-AGCGAGCATCCCCCAAAGTT-3', reverse primer 5'-GGGCACGAAGGCTCATCATT-3') with a product size of 285 bp. Real-time PCR was performed using ABI 7500 and cycle parameters: denaturation at 95°C for 30 s, followed by 40 cycles of 95°C for 5 s, 60°C for 4 s, and 72°C for 30s. The purity of each PCR product was checked by dissociation curve analysis as well as by running the samples on 1% agarose gels. Fold change values were calculated using the formula of $2^{\wedge\triangle\triangle Ct}$.

Western blotting analysis

Cells were harvested and washed in PBS and lysed in extraction buffer containing 1% Nonidet P-40, 0.01% SDS and a protease inhibitor cocktail (Roche, Indianapolis, IN, USA). Protein contents were determined using a BCA assay kit (Pierce, Rockford, IL, USA). Equal amounts of each protein extract (20 μg per lane) were resolved using 10% SDS polyacrylamide gel electrophoresis (SDS-PAGE). Following transblotting onto Immobilon-P membranes (Millipore, Bedford, MA, USA) and blocking with 5% nonfat milk in saline buffer, the membranes were incubated with anti-human Cathepsin V antibody (Cat#: ab166894, Abcam, Cambridge, MA, USA), anti-human Pmel 17/gp100 (Cat# ab137062, Abcam), anti-human tyrosinase (Cat# ab61294, Abcam) at a 1:1,500 dilution, or with an anti-GAPDH antibody (Santa Cruz, Santa Cruz, CA, USA) at a dilution of 1:1,000, for 1 h at room temperature. The membranes were then washed and incubated with HRP-conjugated anti-rabbit IgG (Pierce) at a dilution of 1:2,000 for 1 h at room temperature. Membranes were then washed again and specific bands were visualized using a chemiluminescent reaction (ECL; Amersham, Piscataway, NJ, USA).

CTSV activity assay with fluorogenic peptide substrates

CTSV enzyme activity was estimated using the fluorogenic dipeptide substrate, Z-Leu-Arg-AMC (Enzo Life Sciences Inc., Farmingdale, NY, USA) as previously described [15]. For sample preparation, confluent KCs were collected using a cell scraper and were broken using an ultrasonicator, and then centrifuged (12,000g for 10 min at 4°C), after which the supernatants were collected and stored at −80°C until use. Protein concentrations were determined using a BCA assay kit and were utilized at 10 μg in 100 μL assay buffer (25 mM sodium acetate, 0.1 M NaCl, 5 mM dithiothreitol, pH 5.5). Catalytic activity was monitored by measuring fluorescence from substrate hydrolysis at (excitation 360 nm, emission 460 nm) in a Synergy^{TM} HT Multi-Mode Microplate Reader (BioTek Instruments, Winooski, VT USA) for 30 min at 37°C.

In vitro membrane-toxicity assay by KC lysates or recombinant human CTSV

KCs were seeded at exponential phase in 6-well plates. For UVB irradiation, the medium was changed to warm PBS, and KCs were exposed to 30 mJ/cm^2 UVB. Control cells were mock-irradiated at the same time. For preparation of cell lysates, confluent KCs were collected using a cell scraper, and were prepared by sonication and centrifuged (12,000g for 10 min), and finally the supernatant was stored at −80°C until use [15]. To determine the effect of KC lysates on the melanocore fraction, the purified melanocores were incubated with KC lysates in 500 μl assay buffer (25 mM sodium acetate, 0.1 M NaCl, 5 mM dithiothreitol, pH 5.5) at 37°C for 8 h. Meanwhile, melanocore specimens were also incubated with 1 μg/mL rhCTSV (Cat #: 1080-CY, R&D System, Minneapolis, MN, USA) in assay buffer, which was used as the positive control. After treatment, the samples were washed with 500 μl buffer and centrifuged (2,000 g for 10 min). The pelleted melanocores were immediately fixed with a 2.5% glutaraldehyde solution for analysis by TEM. At least five TEM images were randomly taken of each melanocore specimen. The percentage of damaged melanocores was calculated to represent the efficacy of melanocore degradation.

siRNA-induced CTSV mRNA knockdown

Small interfering RNA (siRNA) duplexes targeting CTSV (Cat#: sc-44526) and a non-targeting scrambled control (Cat#: sc-37007) were purchased from Santa Cruz Biotechnology (Santa Cruz, CA, USA). HaCaT or KCs were seeded in 6-well plates. CTSV siRNA or the scrambled control was mixed with siRNA transfection medium (Cat#: sc-29528, Santa Cruz) and dropped onto the cells according to the manufacturer's instructions. The efficiency of CTSV knockdown by these siRNAs was tested using RT-PCR and western blotting.

Statistical analysis

Data are expressed as means ± SD from at least 3 independent experiments, and SPSS 19.0 version was used to analyze the data. Statistical differences were determined by Student's t-test or one-way analysis of variance (ANOVA). Statistical analyses were performed using GraphPad Prism (San Diego, CA, USA). Asterisks indicate significant differences, $P < 0.05$.

Disclosure of potential conflicts of interest

No potential conflicts of interest were disclosed.

Funding

This work was supported by grants from the National Natural Science Foundation of China (NSFC) [grant numbers 81371717 and 81573028].

Acknowledgments

We thank Dr. Vincent J. Hearing (DASS Manuscript, Haymarket, VA, USA) for valuable discussion and editing of the manuscript.

References

[1] Coelho SG, Yin L, Smuda C, et al. Photobiological implications of melanin photoprotection after UVB-induced tanning of human skin but not UVA-induced tanning. Pigm Cell Melanoma Res. 2015;28:210–216. PMID: 25417821. Available from: http://dx.doi.org/10.1111/pcmr.12331 PMID:25417821.

[2] Milch JM, Logemann NF. Photoprotection prevents skin cancer: Let's make it fashionable to wear sun-protective clothing. Cutis. 2017;99:89–92. PMID:28319625.

[3] Sun X, Kim A, Nakatani M, et al. Distinctive molecular responses to ultraviolet radiation between keratinocytes and melanocytes. Exp Dermatol. 2016;25:708–713. PMID: 27119462. Available from: http://dx.doi.org/10.1111/exd.13057 doi:10.1111/exd.13057. PMID:27119462

[4] Jiang S, Liu XM, Dai X, et al. Regulation of DHICA-mediated antioxidation by dopachrome tautomerase: Implication for skin photoprotection against UVA radiation. Free Radic Biol Med. 2010;48:1144–1151. PMID: 20123016. Available from: http://dx.doi.org/10.1016/j.freeradbiomed.2010.01.033 doi:10.1016/j.freeradbiomed.2010.01.033. PMID:20123016

[5] Hearing VJ. Regulating melanosome transfer: Who's driving the bus? Pigm Cell Res. 2007;20:334–335. PMID: 17850503. Available from: http://dx.doi.org/10.1111/j.1600-0749.2007.00402.x PMID:17850503

[6] Wu X, Hammer JA. Melanosome transfer: It is best to give and receive. Curr Opin Cell Biol. 2014;29:1–7. PMID: 24662021. Available from: http://dx.doi.org/10.1016/j.ceb.2014.02.003 doi:10.1016/j.ceb.2014.02.003. PMID:24662021

[7] Borovanský J, Elleder M. Melanosome degradation: Fact or fiction. Pigm Cell Res. 2003;16:280–286. PMID: 12753402. Available from: http://dx.doi.org/10.1034/j.1600-0749.2003.00040.x doi:10.1034/j.1600-0749.2003.00040.x. PMID:12753402

[8] Ando H, Niki Y, Ito M, et al. Melanosomes are transferred from melanocytes to keratinocytes through the processes of packaging, release, uptake, and dispersion. J Invest Dermatol. 2012;132:1222–1229. PMID: 22189785. Available from: http://dx.doi.org/10.1038/jid.2011.413 doi:10.1038/jid.2011.413. PMID:22189785

[9] Scott G, Deng A, Rodriguez-Burford C, et al. Protease-activated receptor 2, a receptor involved in melanosome transfer, is upregulated in human skin by ultraviolet irradiation. J Invest Dermatol. 2001;117:1412–1420. PMID:11886502. Available from: http://dx.doi.org/10.1046/j.0022-202x.2001.01575.x doi:10.1046/j.0022-202x.2001.01575.x. PMID:11886502

[10] Jimbow K, Sugiyama S. In: Nordlund JJ, Boissy RE, Hearing VJ, King RA, Ortonne JP, editors. The pigmentary system. New York: Oxford University Press; 1998. p. 107–114.

[11] Ortonne JP. Normal and abnormal skin color. Ann Dermatol Venereol. 2012;139:S73–7. PMID: 23260521. Available from: http://dx.doi.org/10.1016/S0151-9638(12)70114-X doi:10.1016/S0151-9638(12)70114-X. PMID:23260521

[12] Correia MS, Moreiras H, Pereira FJC, et al. Melanin transferred to keratinocytes resides in non-degradative endocytic compartments. J Invest Dermatol. 2017;138:637–646. PMID:29074272. Available from: http://dx.doi.org/10.1016/j.jid.2017.09.042 PMID:29074272

[13] Zareba M, Szewczyk G, Sarna T, et al. Effects of photodegradation on the physical and antioxidant properties of melanosomes isolated from retinal pigment epithelium. Photochem Photobiol. 2006;82:1024–1029. PMID: 17205626. Available from: http://dx.doi.org/10.1562/2006-03-08-RA-836 doi:10.1562/2006-03-08-RA-836. PMID:17205626

[14] Nielsen KP, Zhao L, Stamnes JJ, et al. The importance of the depth distribution of melanin in skin for DNA protection and other photobiological processes. J Photochem Photobiol B. 2006;82:194–198. PMID: 16388960. Available from: http://dx.doi.org/10.1016/j.jphotobiol.2005.11.008 doi:10.1016/j.jphotobiol.2005.11.008. PMID:16388960

[15] Ebanks JP, Koshoffer A, Wickett RR, et al. Hydrolytic enzymes of the interfollicular epidermis differ in expression and correlate with the phenotypic difference observed between light and dark skin. J Dermatol. 2013;40:27–33. PMID: 23088390. Available from: http://dx.doi.org/10.1111/j.1346-8138.2012.01634.x doi:10.1111/j.1346-8138.2012.01634.x. PMID:23088390

[16] Chen N, Seiberg M, Lin CB. Cathepsin L2 levels inversely correlate with skin color. J Invest Dermatol. 2006;126:2345–2347. PMID: 16728970. Available from: http://dx.doi.org/10.1038/sj.jid.5700409 doi:10.1038/sj.jid.5700409. PMID:16728970

[17] Tarafder AK, Bolasco G, Correia MS, et al. Rab11b mediates melanin transfer between donor melanocytes and acceptor keratinocytes via coupled exo/endocytosis. J Invest Dermatol. 2014;134:1056–1066. PMID:24141907. Available from: http://dx.doi.org/10.1038/jid.2013.432 doi:10.1038/jid.2013.432. PMID:24141907

[18] Hurbain I, Romao M, Sextius P, et al. Melanosome distribution in keratinocytes in different skin types: Melanosome clusters are not degradative organelles. J Invest Dermatol. 2017;138:647–656. PMID:29054596. Available from: http://dx.doi.org/10.1016/j.jid.2017.09.039 PMID:29054596

[19] Peles DN, Simon JD. The ultraviolet absorption coefficient of melanosomes decreases with increasing pheomelanin content. J Phys Chem B. 2010;114:9677–9683. PMID:20614877. Available from: http://dx.doi.org/10.1021/jp102603b doi:10.1021/jp102603b. PMID:20614877

[20] Liu XM, Zhou Q, Xu SZ, et al. Maintenance of immune hyporesponsiveness to melanosomal proteins by DHICA-mediated antioxidation: Possible implications for autoimmune vitiligo. Free Radic Biol Med. 2011;50:1177–1185. PMID:21256957. Available from: http://dx.doi.org/10.1016/j.freeradbiomed.2011.01.017 doi:10.1016/j.freeradbiomed.2011.01.017. PMID:21256957

[21] Murase D, Hachiya A, Takano K, et al. Autophagy has a significant role in determining skin color by regulating melanosome degradation in keratinocytes. J Invest Dermatol. 2013;133:2416–2424. PMID: 23558403. Available from: http://dx.doi.org/10.1038/jid.2013.165 doi:10.1038/jid.2013.165. PMID:23558403

[22] Hu QM, Yi WJ, Su MY, et al. Induction of retinal-dependent calcium influx in human melanocytes by UVA or UVB radiation contributes to the stimulation of melanosome transfer. Cell Prolif. 2017;50:e12372. PMID: 28833830. Available from: http://dx.doi.org/10.1111/cpr.12372 doi:10.1111/cpr.12372.

[23] Luo L F, Shi Y, Zhou Q, et al. Insufficient expression of the melanocortin-1 receptor by human dermal fibroblasts contributes to excess collagen synthesis in keloid scars. Exp Dermatol. 2013;22:764–766. PMID:24433185. Available from: http://dx.doi.org/10.1111/exd.12250 doi:10.1111/exd.12250. PMID:24433185

[24] Lichti U, Anders J, Yuspa S H. Isolation and short-term culture of primary keratinocytes, hair follicle populations and dermal cells from newborn mice and keratinocytes from adult mice for in vitro analysis and for grafting to immunodeficient mice. Nat Protoc. 2008;3:799–810. PMID:18451788. Available from: http://dx.doi.org/10.1038/nprot.2008.50 doi:10.1038/nprot.2008.50. PMID:18451788

[25] Kushimoto T, Basrur V, Valencia J, et al. A model for melanosome biogenesis based on thepurification and analysis of early melanosomes. Proc Natl Acad Sci U S A. 2001;98:10698–10703. PMID: 11526213. Available from: http://dx.doi.org/10.1073/pnas.191184798 doi:10.1073/pnas.191184798. PMID:11526213

[26] Ando H, Niki Y, Ito M, et al. Melanosomes are transferred from melanocytes to keratinocytes through the processes of packaging, release, uptake, and dispersion. J Invest Dermatol. 2012;132:1222–1229. PMID: 22189785. Available from: http://dx.doi.org/10.1038/jid.2011.413 doi:10.1038/jid.2011.413. PMID:22189785

[27] Ando H, Niki Y, Yoshida M, et al. Involvement of pigment globules containing multiple melanosomes in the transfer of melanosomes from melanocytes to keratinocytes. Cell Logist. 2011;1:12–20. PMID: 21686100. Available from: http://dx.doi.org/10.4161/cl.1.1.13638 doi:10.4161/cl.1.1.13638. PMID:21686100

[28] Ebanks JP, Koshoffer A, Wickett RR, et al. Epidermal keratinocytes from light vs. dark skin exhibit differential degradation of melanosomes. J Invest Dermatol. 2011;131:1226–1233. PMID: 21326292. Available from: http://dx.doi.org/10.1038/jid.2011.22 doi:10.1038/jid.2011.22. PMID:21326292

[29] Choi HI, Sohn KC, Hong DK, et al. Melanosome uptake is associated with the proliferation and differentiation of keratinocytes. Arch Dermatol Res. 2014;306:59–66. PMID: 24173125. Available from: http://dx.doi.org/10.1007/s00403-013-1422-x doi:10.1007/s00403-013-1422-x. PMID:24173125

[30] Miao F, Shi Y, Fan ZF, et al. Deoxyarbutin possesses a potent skin-lightening capacity with no discernible cytotoxicity against melanosomes. PLoS One. 2016;11:e0165338. PMID: 27776184. Available from: http://dx.doi.org/10.1371/journal.pone.0165338 doi:10.1371/journal.pone.0165338. PMID:27776184

[31] Zhang J, Wu J, Yang L, et al. DNA damage in lens epithelial cells and peripheral lymphocytes from age-related cataract patients. Ophthal Res. 2014;51:124–128. PMID: 24457594. Available from: http://dx.doi.org/10.1159/000356399 doi:10.1159/000356399. PMID:24457594

[32] Thompson BC, Halliday GM, Damian DL. Nicotinamide enhances repair of arsenic and ultraviolet radiation-induced DNA damage in HaCaT keratinocytes and ex vivo human skin. PLoS One. 2015;10:e0117491. PMID: 25658450. Available from: http://dx.doi.org/10.1371/journal.pone.0117491 doi:10.1371/journal.pone.0117491. PMID:25658450

[33] Shi Y, Luo LF, Liu XM, et al. Premature graying as a consequence of compromised antioxidant activity in hair bulb melanocytes and their precursors. PLoS One. 2014;9:e93589. PMID:24695442. Available from: http://dx.doi.org/10.1371/journal.pone.0093589 doi:10.1371/journal.pone.0093589. PMID:24695442